BUBBLE SUSPENSION RHEOLOGY AND IMPLICATIONS FOR CONDUIT-FLOW

E. W. LLEWELLIN AND M. MANGA

Abstract. Bubbles are ubiquitous in magma during eruption and have a profound impact on its rheology. Despite this, bubble-suspension rheology is routinely ignored in conduit flow and eruption models, potentially impairing accuracy and resulting in the loss of important phenomenological richness. The omission is due, in part, to a historical confusion in the literature concerning the effect of bubbles on the rheology of a liquid. This confusion has now been largely resolved and recently-published studies have identified two viscous regimes: in regime 1, the viscosity of the two-phase (magma–gas) suspension increases as gas volume fraction ϕ increases; in regime 2, the viscosity of the suspension decreases as ϕ increases. The viscous regime for a deforming bubble suspension can be determined by calculating two dimensionless numbers, the capillary number Ca and the dynamic capillary number Cd.

This paper provides a didactic explanation of how to include the effect of bubble-suspension rheology in conduit flow models. Recent published work on bubble-suspension rheology is reviewed and a practical rheological model is presented and justified followed by an algorithmic, step-by-step guide to including the rheological model in conduit flow models. Preliminary results from conduit flow models which have implemented the model presented are discussed and it is concluded that the effect of bubbles on magma rheology is important in nature and results in a decrease of at least 800m in fragmentation depth and an increase of at least 20% in eruption rate compared with the assumption of Newtonian rheology.

1. Introduction

The region between bubble nucleation and magma fragmentation in the volcanic conduit is characterized by the flow of a two-phase suspension of bubbles in magma (suspended crystals may also be present but are not considered in this paper). It is known from theory (e.g., Taylor, 1932; Mackenzie, 1950; Frankel and Acrivos, 1970), laboratory experiments (Bagdassarov and Dingwell, 1992, 1993; Stein and Spera, 1992, 2002; Lejeune *et al.*, 1999; Rust and Manga, 2002a; Llewellin *et al.*, 2002a), and numerical simulations (e.g., Manga *et al.*, 1998; Manga and Loewenberg, 2001) that bubbles influence the rheology of the suspension. In particular, it is likely that the influence of bubbles on the shear viscosity of the magma ($\eta_s(\phi)$ where η_s is the viscosity of the bubble suspension and ϕ is the gas volume fraction) is an important control on conduit flow and eruption dynamics. Despite this there has, until recently, been very little effort to include bubble suspension rheology in numerical conduit flow models (but see Mastin (2002) for a counter-example). This is due, primarily, to two historical deficiencies in the literature: 1) published equations for $\eta_s(\phi)$ divide into two approximately equally-sized groups, one asserting that η_s increases with increasing ϕ, the other that η_s decreases with increasing ϕ; 2) within each group there is little consensus on the functional form of $\eta_s(\phi)$. Since

2002, several papers have been published which have addressed both of these deficiencies. Critically, the apparent confusion over the sign of $\eta_{\rm s}(\phi)$ has been resolved: bubbles can either increase or decrease the shear viscosity of a suspension depending on the dynamic regime (Llewellin *et al.*, 2002a,b; Rust and Manga, 2002a; Stein and Spera, 2002). In addition, each of these studies added new experimental data allowing the functional form of $\eta_{\rm s}(\phi)$ to be more tightly constrained.

Given these advances, it is now possible and desirable to include bubble-suspension rheology in conduit flow and eruption models. The main purpose of this paper is to present an algorithmic approach to accounting for bubble-suspension rheology in such models—this is intended as a 'how to' guide for modellers. Additionally, the paper includes a brief review of bubble-suspension rheology with a particular emphasis on clarifying the recent advances mentioned above. Some models described elsewhere in this volume have already implemented the algorithm presented in this paper and we show some preliminary results from these models which give an indication of the effect that including bubble-suspension rheology has on conduit flow and eruption models.

2. Bubble suspension rheology

The rheological, bubble suspension property of greatest importance in conduit flow is its shear viscosity $\eta_{\rm s}$. This is typically normalized to the viscosity of the liquid phase μ_0 and presented as the relative viscosity $\eta_{\rm r}$:

$$\eta_{\rm r} = \frac{\eta_{\rm s}}{\mu_0}. \tag{1}$$

$\eta_{\rm r}$ is a function of ϕ, the sign of which depends on the conditions of shear and the bubble-relaxation time λ. λ is a measure of the timescale over which a bubble can respond to changes in its shear environment. For a single bubble in an infinite medium:

$$\lambda = \frac{\mu_0 a}{\Gamma} \tag{2}$$

where a is the undeformed bubble radius and Γ is the bubble–liquid interfacial tension. There is some evidence that λ is an increasing function of ϕ (Oldroyd, 1953; Oosterbroek and Mellema, 1981; Loewenberg and Hinch, 1996; Llewellin *et al.*, 2002a), however, Rust *et al.* (2003) show that the dependence of λ on ϕ is rather weak so, for simplicity, it is proposed that equation 2 is used for all ϕ. Other aspects of the suspension rheology are also strongly influenced by the presence of bubbles. For example, viscoelastic effects, including recoverable strain are introduced, in addition, normal stress differences are generated even if the suspending liquid is Newtonian (e.g., Schowalter et al., 1968; Stein and Spera, 1992; Manga et al., 1998). Such effects are not considered further in this paper.

The algorithm for including bubble-suspension rheology in conduit flow models which is presented later in section 3 depends upon distinguishing the two dynamic regimes for $\eta_{\rm r}(\phi)$. We identify:

Regime 1: shear viscosity increases with increasing gas volume-fraction.
Regime 2: shear viscosity decreases with increasing gas volume-fraction.

The regime can be determined by calculating the capillary number Ca for a steady flow (Llewellin *et al.*, 2002b; Rust and Manga, 2002a; Stein and Spera, 2002) or the dynamic capillary number Cd for an unsteady flow (Llewellin *et al.*, 2002a,b) as described in detail below.

2.1. **Steady flows.** Strictly, a flow is described as steady if the conditions of shear have remained constant (in the Lagrangian sense) for a time before present $t \gg \lambda$ (Llewellin *et al.*, 2002a; Rust and Manga, 2002b). This definition is loosened somewhat in section 2.2. Manga and Loewenberg (2001), Llewellin *et al.* (2002b), Rust and Manga (2002a) and Stein and Spera (2002) show that, for a steady flow, the viscous regime is controlled by the capillary number Ca, given by:

$$Ca = \lambda\dot{\gamma} \tag{3}$$

where $\dot{\gamma}$ is the shear strain rate. Ca describes the relative importance of viscous stresses (of order $\mu_0\dot{\gamma}$) , which tend to deform the bubbles, and interfacial stresses (of order Γ/a), which tend to restore them to sphericity. Since the flow is steady, Ca refers to the *equilibrium* between these forces, hence, the bubble shape is also stable (bubbles are described as relaxed) and is referred to as the *equilibrium deformation*. The magnitude of equilibrium bubble-deformation, therefore, depends on Ca. If $Ca \ll 1$, interfacial tension forces dominate and bubbles are approximately spherical (e.g., Taylor, 1934). If $Ca \gg 1$, viscous forces dominate and bubbles will be elongate (e.g. Hinch and Acrivos, 1980). The effect of bubble shape on viscosity can be explained as follows: Bubbles deform flow lines within the suspending medium, which tends to increase viscosity; bubbles provide free-slip surfaces within the suspending medium, which tends to decrease viscosity. For small Ca (bubbles are almost spherical) flow-line distortion is great and free-slip surface area is small, hence, $\eta_\mathrm{r} > 1$; for large Ca (bubbles are elongate) flow-line distortion is small and free-slip surface area is great, hence, $\eta_\mathrm{r} < 1$.

In summary: $Ca \ll 1$ denotes regime 1; $Ca \gg 1$ denotes regime 2.

In principle, if the shape of bubbles can be determined as a function of Ca and ϕ then the rheology of the suspension can predicted (e.g., Batchelor, 1970). The problem, however, lies in determining bubble shape. For dilute suspensions, analytical results are available for small deformations (e.g., Taylor, 1934) and highly elongate bubbles (e.g., Acrivos and Hinch, 1980). Models are also derived for intermediate deformation (e.g., Wu et al., 2002). In general theoretical results for bubble shape agree well with experimental measurements (e.g., Rust and Manga, 2002b; Hu and Lips, 2003; Yu and Bousmina, 2003). When the suspension is no longer dilute, however, the interactions between bubbles affect their shapes and consequently the rheology. Unfortunately, the rheology can be predicted accurately only if the bubble shape is accurately known (Cristini et al., 2002).

2.2. **Unsteady flows.** Given the definition of a steady flow at the beginning of section 2.1, it is clear that if the shear strain-rate is changing, the flow must be unsteady. In fact, Llewellin *et al.* (2002a,b) have shown that there are degrees of steadiness of flow which can be described using the dynamic capillary number Cd, given by:

$$Cd = \lambda\frac{\ddot{\gamma}}{\dot{\gamma}} \tag{4}$$

where $\ddot{\gamma}$ is the rate of change of shear strain-rate. Cd compares the timescale over which the bubbles can respond to changes in their shear environment (the bubble-relaxation time λ) with the timescale over which the shear environment changes (of order $\dot{\gamma}/\ddot{\gamma}$). If $Cd \ll 1$, the bubbles are able to respond continuously to the changes in shear environment. Consequently, the bubbles are always approximately in their equilibrium deformation and the flow is approximately steady. Since the flow is

approximately steady, the dynamic regime is controlled by the capillary number Ca as described in section 2.1. If, however, $Cd \gg 1$, the shear environment is changing too rapidly for the bubbles to respond, therefore the bubbles are unrelaxed. Since the bubbles never reach their equilibrium deformation, Ca is undefined and the flow is described as *unsteady*. In an unsteady flow, the bubbles do not have time to respond elastically to changes in shear, hence, they behave as if they have no bubble–liquid interfacial tension and deform passively with the suspending liquid. This decreases the distortion of flow-lines around the bubbles leading to a decrease in the viscosity of the suspension as ϕ increases (Llewellin *et al.*, 2002a).
In summary: $Cd \ll 1$ flow is approximately steady so regime is determined by considering Ca; $Cd \gg 1$ denotes regime 2.

Just as rheology can be calculated from knowledge of bubble shapes for steady flows, so too can the rheology for unsteady flows if the evolution of bubble shape is known (e.g., Tucker and Moldenaers, 2002). Several recent studies have made progress in developing models for the time-dependent deformation of bubble shape and rheology in a variety of flow geometries (e.g., Maffettone and Minale, 1998; Jansseune et al., 2001; Jackson and Tucker, 2003; Yu and Bousmina, 2003).

2.3. **Proposed rheological model.** There are nine published datasets from laboratory experiments on bubble suspensions (Rahaman, 1987; Ducamp and Raj, 1989; Bagdassarov and Dingwell, 1992, 1993; Stein and Spera, 1992, 2002; Lejeune *et al.*, 1999; Llewellin *et al.*, 2002a; Rust and Manga, 2002a). Of these, unsteady flows are considered explicitly in the studies of Bagdassarov and Dingwell (1993) and Llewellin *et al.* (2002a). From the published experimental details it is possible to deduce that the data presented in Rahaman (1987, Ducamp and Raj (1989), Bagdassarov and Dingwell (1992), Lejeune *et al.* (1999), and Stein and Spera (2002) where collected from unsteady flows. Rust and Manga (2002a) explicitly considered steady flow. In addition, there are two published datasets from numerical models of bubble suspensions (Manga *et al.*, 1998; Manga and Loewenberg, 2001). Many of the papers mentioned above present models for $\eta_\mathrm{r}(\phi)$ based on their experimental data. These and other models are discussed in detail in Llewellin *et al.* (2002a).

From the published data it is evident that $\eta_\mathrm{r}(\phi)$ is largely independent of Cx (where Cx represent either Ca or Cd) when $Cx \ll 1$ and $Cx \gg 1$. $\eta_\mathrm{r}(\phi)$ is strongly dependent on Cx only in the narrow region where the dynamic regime changes ($Cx \approx O(1)$). Additionally, in this region, no easily-evaluated equation for $\eta_\mathrm{r}(\phi, Cx)$ has been published (e.g., Yu and Bousmina). For these reasons, we propose that $\eta_\mathrm{r}(\phi, Cx)$ should be treated as a step-function, with one equation for $\eta_\mathrm{r}(\phi)$ used for $Cx \leq 1$ (regime 1) and another equation for $\eta_\mathrm{r}(\phi)$ used for $Cx > 1$ (regime 2). This approach significantly simplifies the task of including bubble-suspension rheology in numerical models whilst retaining its most important features. An indication of the size of the error in η_r which is introduced in the region where $Cx \approx O(1)$ by this approximation is presented in figure 1, which compares the curve of $\eta_\mathrm{r}(Ca)$ (for $\phi = 0.4$ and steady flow) produced by the "model 4" of Pal (2003) (presented below as equation 5) and the simplified model proposed in this paper. It is argued that the residual is acceptable when it is considered that, in a volcanic eruption, values of Cx will span many orders of magnitude and the transition through $Cx \approx O(1)$ is likely to be very rapid in space and time.

Llewellin *et al.* (2002b) show that $\eta_\mathrm{r}(\phi, Ca)$ and $\eta_\mathrm{r}(\phi, Cd)$ are identical (that is, the dependence of shear viscosity on gas volume-fraction is identical for both steady

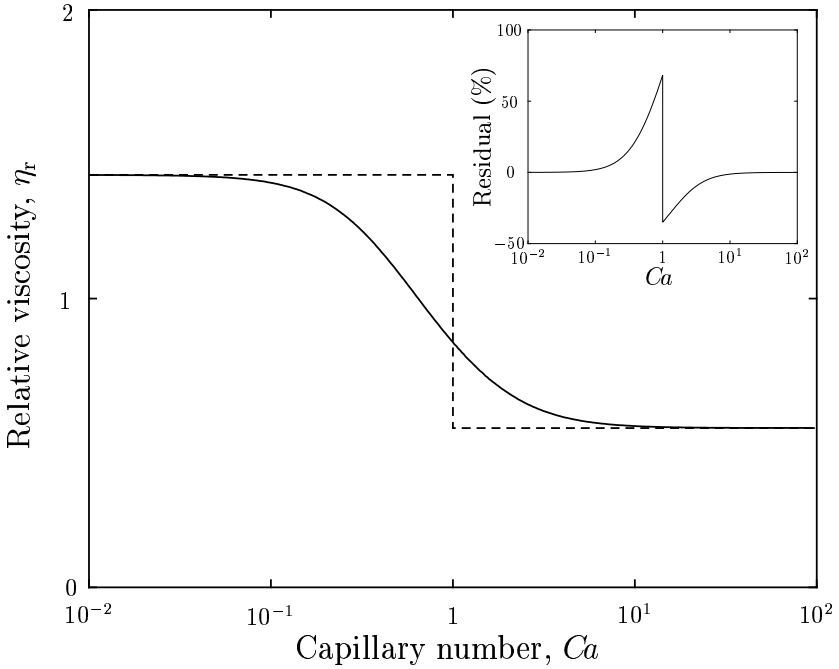

FIGURE 1. Comparison of $\eta_r(Ca)$ calculated using "model 4" of Pal (2003) (solid line) and using the simplified model proposed in this paper (dashed line) for $\phi = 0.4$. Inset shows residual as a percentage of the value calculated using Pal's equation.

and unsteady flows) except for a very small deviation when $Cx \approx 1$. We propose, therefore, that a single equation for the positive dependence of η_r on ϕ is used for regime 1 and a single equation for the negative dependence of η_r on ϕ is used for regime 2, regardless of whether regime 2 behaviour is due to $Ca > 1$ (for a steady flow) or $Cd > 1$ (for an unsteady flow).

We must now choose an equation for $\eta_r(\phi)$ to be used for regime 1 and another for regime 2. Pal (2003) presents four semi-empirical models for $\eta_r(\phi, Ca)$ for steady flows, parameterized using previously-published data for the rheology of bubble suspensions. He obtains the best fit to data using his "model 4":

$$\eta_r \left(\frac{1 - \frac{12}{5}\eta_r^2 Ca^2}{1 - \frac{12}{5}Ca^2} \right)^{-\frac{4}{5}} = \left(1 - \frac{\phi}{\phi_m} \right)^{-\phi_m} \tag{5}$$

where ϕ_m is the maximum packing fraction of bubbles. This model is an extension, after the method of Brinkman (1952) and Roscoe (1952), of the Frankel and Acrivos (1970) model for non-dilute suspensions The introduction of a maximum packing fraction (by analogy with the Brinkman-Roscoe method for suspensions of solid particles) is somewhat problematic: since bubbles are deformable, no clear maximum packing fraction exists (except, perhaps, $\phi_m = 1$), additionally, no real solution to equation 5 exists for $1 > \phi \geqslant \phi_m$. The most reasonable solution is always to set $\phi_m = 1$. In this case, for the limits of large and small Ca, equation 5

reduces to:

$$\eta_{\mathrm{r}} = \begin{cases} (1-\phi)^{-1} & : \quad Ca \ll 1 \\ (1-\phi)^{\frac{5}{3}} & : \quad Ca \gg 1. \end{cases} \tag{6}$$

Pal's model does not consider the steadiness of the flow, a property which has been shown by Llewellin *et al.* (2002a,b) to be a fundamental control on the rheology of a bubble suspension in the flows that arise in volcanic conduits. However, since Llewellin *et al.* (2002b) also show that $\eta_{\mathrm{r}}(\phi, Cx)$ is almost identical for steady and unsteady flows it is reasonable to assume that equation 6 has equal validity for unsteady flows (with Cd replacing Ca for each regime).

For experimental and numerical investigations of bubble suspensions in regime 1: equation 6 agrees reasonably well with Manga *et al.* (1998), Rust and Manga (2002a) and with Llewellin *et al.* (2002a) for $0 < \phi < 0.07$. The model is incompatible with data from Llewellin *et al.* (2002a) for $\phi > 0.07$ or Stein and Spera (1992), both of which indicate a much stronger positive dependence of η_{r} on ϕ than predicted by Pal's model.

For experimental and numerical investigations of bubble suspensions in regime 2: equation 6 agrees reasonably well with Lejeune *et al.* (1999), Manga and Loewenberg (2001), Stein and Spera (2002) and Llewellin *et al.* (2002a), most of whom considered simple shearing flows. The model is incompatible with data from sintering experiments and extensional flows (Rahaman, 1987; Ducamp and Raj, 1989; Bagdassarov and Dingwell, 1992), all of which indicate a much stronger negative dependence of η_{r} on ϕ than predicted by Pal's model. Possibly a volume change in these latter experiments may have influenced their results.

It is clear from the above that the "model 4" proposed by Pal does not encapsulate the behaviour identified in several experimental studies of bubble suspension behaviour. However, it does capture the broad trends which exist in all of the data in both regimes, for measurements on both steady and unsteady flows. In addition, the model tends to underestimate the importance of bubbles in controlling the shear viscosity of a suspension in both regimes. The model can, therefore, be usefully employed as a "minimum" model of bubble rheology and the effect of bubbles on conduit flow dynamics in the real world will be *at least* as great as any effect identified using a conduit flow model which incorporates the effect of bubbles on rheology using this model. Bearing in mind the simplifying assumption, presented above, that regime 1 extends to $Cx \leq 1$ and regime 2 from $Cx > 1$, we, therefore, propose the following minimum model of bubble-suspension rheology for use in conduit flow models:

$$\text{Regime 1 (min.)} : \quad \eta_{\mathrm{r}} = (1-\phi)^{-1}, \tag{7}$$

$$\text{Regime 2 (min.)} : \quad \eta_{\mathrm{r}} = (1-\phi)^{\frac{5}{3}}. \tag{8}$$

Note that equations 7 and 8 reduce to the exact analytical results for dilute ($\phi \ll 1$) suspensions for both regime 1 (Taylor, 1932) and regime 2 (Mackenzie, 1950).

It is also of interest to investigate a "maximum" model of bubble rheology, based on models for behaviour in regimes 1 and 2 proposed by those workers who find a stronger dependence of η_{r} on ϕ than is predicted by equations 7 and 8. For regime 1, the strongest dependence is proposed by Llewellin *et al.* (2002a):

$$\text{Regime 1 (max.)} : \quad \eta_{\mathrm{r}} = 1 + 9\phi. \tag{9}$$

This relationship is based on experiments on bubble suspensions in the range $0 \leqslant \phi \leqslant 0.5$. For regime 2, we propose that the model presented by Bagdassarov and Dingwell (1992) is used:

$$\text{Regime 2 (max.)}: \quad \eta_{\mathrm{r}} = \frac{1}{1 + 22.4\phi}. \tag{10}$$

This equation is based on measurements of bubble suspensions in the range $0 \leqslant \phi \leqslant 0.7$. It is probable that the true effect of bubbles on conduit flow dynamics will be somewhere between that predicted using the "minimum" and "maximum" models presented above.

3. Implementation of bubble suspension rheology

We propose that conduit flow models incorporate the effect of bubbles on rheology by first calculating the dynamic regime of the flow in each conduit element, then calculating the viscosity of the material in that conduit element using equation 7 for flows in regime 1 and equation 8 for flows in regime 2 when using the minimum model and equations 9 and 10 when the "maximum" model is employed—see section 2.3. The procedure is summarized in figure 2. It is envisaged that the viscosity determination will occur at the end of each timestep for each conduit element. The resulting viscosity value will then be used to determine the velocity profile in the next timestep.

To calculate Ca (equation 3) and Cd (equation 4), the relaxation time λ, the shear strain-rate $\dot{\gamma}$ and the rate of change of shear strain-rate $\ddot{\gamma}$ must first be calculated. The remainder of this section describes how these quantities may be calculated for a one-dimensional conduit flow model.

3.1. **Calculating the relaxation time λ.**

Relaxation time is given by equation 2, represented below for convenience:

$$\lambda = \frac{\mu_0 a}{\Gamma}.$$

Due to decompressive and diffusive growth of bubbles, λ changes over time as a packet of magma ascends, hence it must be calculated for each element at each timestep. μ_0 is the viscosity of the liquid part of the two-phase material at that point (usually calculated from composition and temperature of the silicate melt). Γ is the liquid–bubble interfacial tension at that point; a value of $\Gamma \approx 0.25$ N m^{-1} can be deduced from figure 31 of Murase and McBirney (1973).

a, the undeformed bubble radius (the radius of a spherical bubble of equal volume), may be calculated explicitly in some conduit flow models, but not in others. If a is ordinarily calculated, the value appropriate for that element at that timestep should be used. If a is not ordinarily calculated, it may be determined from the gas volume-fraction by assuming a bubble number-density at nucleation (see table of model parameters elsewhere in this volume) and assuming some function for bubble number-density with time: e. g. bubble number-density (with respect to the volume of the *liquid* part of the suspension) over time remains constant.

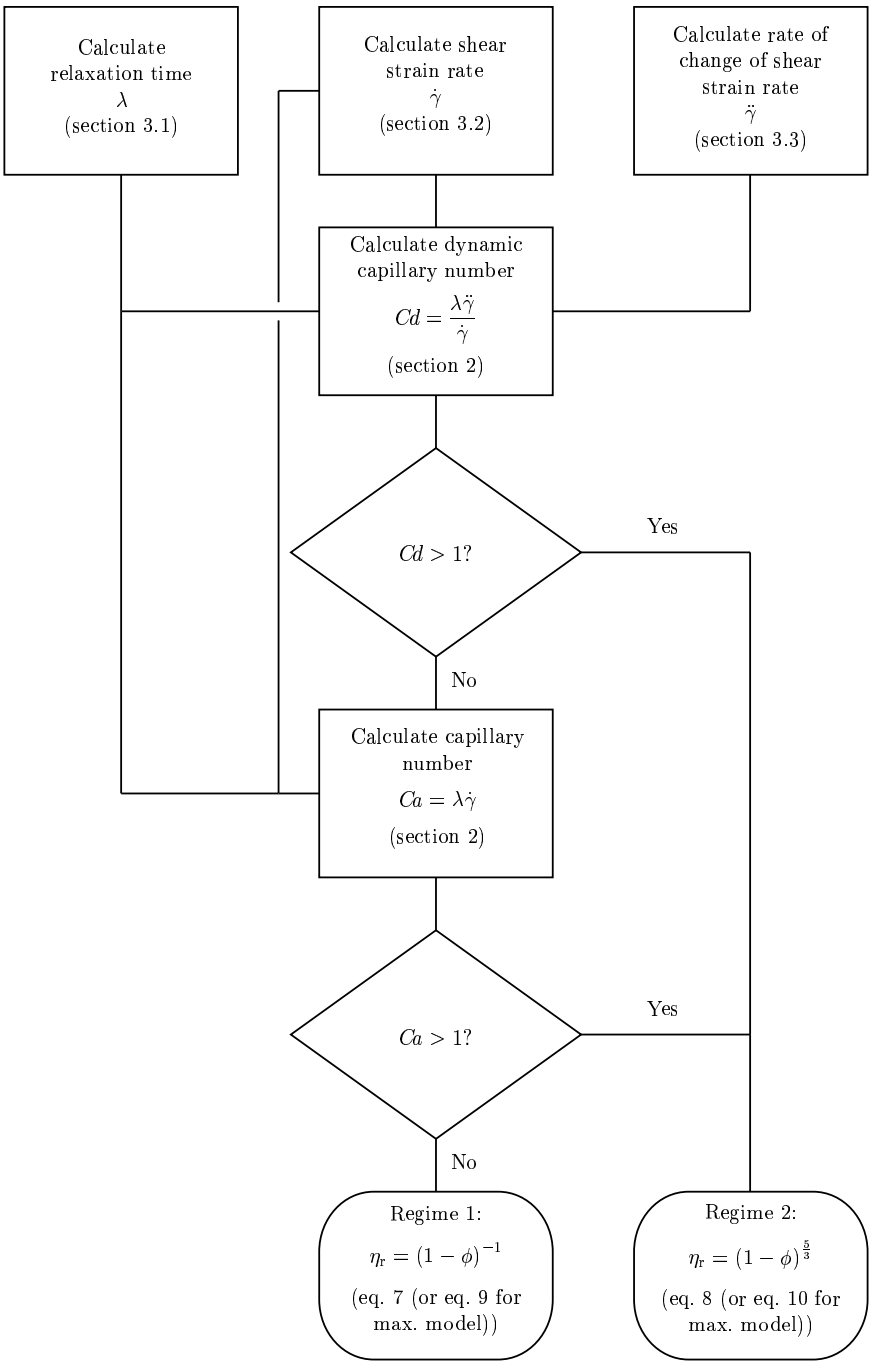

FIGURE 2. Flowchart showing algorithm for determination of shear viscosity for each conduit element. Comments in brackets refer to sections and equations in the main body of these notes. For explanation of "maximum" models, see section 2.3.

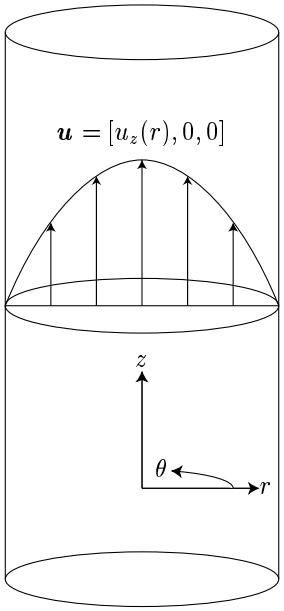

FIGURE 3. Conduit flow.

3.2. **Calculating the shear strain rate $\dot{\gamma}$.**

The shear strain-rate must be calculated for each element at each timestep. For laminar, uniaxial flow along a conduit, the velocity $\boldsymbol{u} = [u_z(r), 0, 0]$ as shown in figure 3. For such a flow, the shear strain-rate is given by:

$$\dot{\gamma} = \frac{\mathrm{d}u_z}{\mathrm{d}r} \tag{11}$$

hence shear strain-rate is a function of radial position in the conduit. It is not possible to calculate $u_z(r)$ using a one-dimensional conduit flow model so, in order to calculate $\dot{\gamma}$, a velocity profile must be assumed.

For slow, steady flows, the shear strain-rate will be low at all points across the conduit, hence $Ca < 1$ everywhere. The viscosity of the bubble suspension will, consequently, be the same everywhere so the velocity profile will be parabolic (the bubble suspension will behave as a Newtonian liquid with a viscosity given by the equation for regime 1 (equation 7, min. model, or 9, max. model). For a parabolic velocity profile, the shear strain-rate varies from zero at the axis to a maximum at the conduit wall. For a bubble suspension, this leads to an interesting phenomenon as the flow rate increases: whilst the shear strain-rate at the axis remains low (hence $Ca < 1$), the shear strain-rate near the conduit wall may increase to the point where $Ca > 1$. In this configuration, at all points axial of the transition, the viscosity of the bubble suspension will be given by the equation for regime 1 but, radially outwards from the transition, the viscosity will be lower, given by the equation for regime 2 (equation 8, min. model, or 10, max. model). This leads to a non-parabolic velocity profile as shown in Llewellin *et al.* (2002b). At still higher flow rates, the shear strain-rate across most of the conduit is such that $Ca > 1$ except for a narrow region near the axis and the velocity profile is, again,

approximately parabolic. Unfortunately, this transitional behaviour can only be captured by 2d and 3d flow models, however, Llewellin *et al.* show that significant departure from parabolic flow occurs only for a narrow range of conditions, hence it is reasonable, for the purposes of this exercise, to assume that the velocity profile in the conduit is always parabolic.

Given a parabolic velocity profile, it is possible to calculate an average shear-strain-rate in terms of the volume flow rate Q, the average velocity $\hat{u}_z$ or the axial velocity u_0 (depending on which is calculated by the conduit flow model). The average shear-strain-rate can then be used to calculate the capillary number and hence the viscosity of the bubble suspension under those conditions of shear.

Assuming a parabolic velocity profile across the conduit we obtain:

$$u_z = u_0 \left(1 - \frac{r^2}{R^2}\right). \tag{12}$$

Where r is the radial position in the conduit and R is the radius of the conduit (assuming no slip at the conduit wall: $u_z = 0$ at $r = R$). Integrating across the conduit gives the volume flow rate:

$$Q = 2\pi u_0 \int_0^R r \left(1 - \frac{r^2}{R^2}\right) \mathrm{d}r \tag{13}$$

hence

$$u_0 = \frac{2Q}{\pi R^2}. \tag{14}$$

Volume flow-rate is the product of the average velocity and the cross-sectional area of the conduit, hence:

$$\hat{u}_z = \frac{Q}{\pi R^2}. \tag{15}$$

We can see from equations 14 and 15 that the axial velocity for parabolic flow along a pipe is twice the average velocity:

$$u_0 = 2\hat{u}_z. \tag{16}$$

Substituting equation 14 into equation 12:

$$u_z = \frac{2Q}{\pi R} \left(1 - \frac{r^2}{R^2}\right). \tag{17}$$

Applying equation 11 to the above we obtain the shear strain-rate as a function of radial position in the conduit:

$$\dot{\gamma} = \frac{4\hat{u}_z r}{R^2}. \tag{18}$$

Integrating across the conduit and dividing by the cross sectional area, we obtain the average shear strain-rate:

$$\hat{\dot{\gamma}} = \frac{8\hat{u}_z}{R^4} \int_0^R r^2 \, \mathrm{d}r \tag{19}$$

which, using equations 15 and 16, can be expressed in terms of the average velocity, the axial velocity or the volume flow-rate, hence, the shear strain-rate can be calculated for each conduit element (the $\hat{}$ is dropped for convenience):

$$\dot{\gamma} = \frac{8u_z}{3R} = \frac{4u_0}{3R} = \frac{8Q}{3\pi R^3}. \tag{20}$$

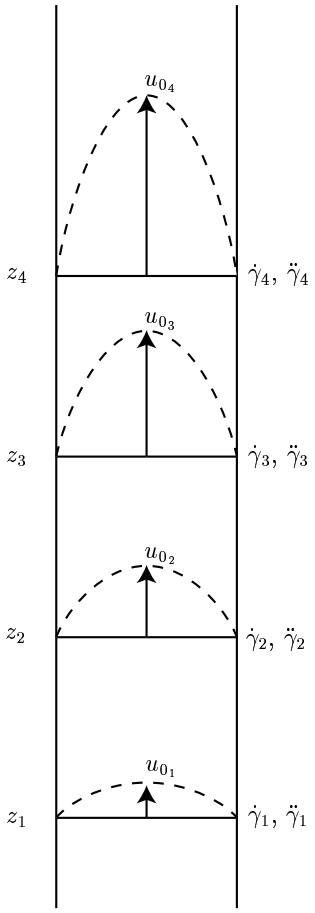

FIGURE 4. Conduit elements.

3.3. **Calculating the rate of change of shear strain-rate $\ddot{\gamma}$.**

The rate of change of shear strain-rate must be calculated for each element at each timestep. Note that this is the rate of change of shear strain-rate experienced by a packet of the magma as it rises up the conduit hence, even for a 'steady' model in which the velocity profile up the conduit does not change with time, the shear strain-rate experienced by a rising packet of magma does change over time.

$\ddot{\gamma}$ can be estimated by considering the strain rate in adjacent elements of the conduit (figure 4). It is assumed that, for each element i of the flow, at depth z_i, the axial velocity u_{0_i} (or the average velocity $\hat{u}_i$ or the volume flow-rate Q_i—see equation 20) is known, hence, the shear strain-rate $\dot{\gamma}_i$ can be calculated according to the method described in section 3.2. The rate of change of shear strain-rate for a packet of material is approximately given by:

$$\ddot{\gamma} \approx \frac{\Delta\dot{\gamma}}{\Delta t} \tag{21}$$

where $\Delta\dot{\gamma}$ is the change in shear strain-rate experienced by the packet over time Δt. In figure 4 material at element i is arriving from element $i-1$, hence it has experienced a change in shear strain-rate given by:

$$\Delta\dot{\gamma}_i = \dot{\gamma}_i - \dot{\gamma}_{i-1}. \tag{22}$$

The time taken for the material to undergo this change is approximately the quotient of the distance between the elements and the average flow velocity between the elements:

$$\Delta t = \frac{2(z_i - z_{i-1})}{\hat{u}_i + \hat{u}_{i-1}} \tag{23}$$

hence:

$$\ddot{\gamma}_i \approx \frac{(\dot{\gamma}_i - \dot{\gamma}_{i-1})(\hat{u}_i + \hat{u}_{i-1})}{2(z_i - z_{i-1})} \tag{24}$$

where all quantities are evaluated in the current timestep and where the average velocity can be derived from the axial velocity or the volume flow-rate using equations 15 and 16. The dynamic capillary number for element i is, therefore, given by:

$$Cd_i = \lambda\frac{\ddot{\gamma}_i}{\dot{\gamma}_i}. \tag{25}$$

At the base of the conduit, $u_{0_0} = \dot{\gamma}_0 = \ddot{\gamma}_0 = 0$.

4. Volcanological implications of including bubble-suspension rheology

Our proposed model implies that for a gas volume-fraction of $\phi < 0.5$, η_r can change by up to a factor of 5 for the minimum model and a factor of 70 for the maximum model. The magnitude of this effect is thus small compared to viscosity changes that ascending magmas can experience due to crystallization and the loss of volatiles. Nevertheless, there is some preliminary evidence that the change in viscosity due to the presence of bubbles has a significant effect on the predictions of conduit flow models. In figure 5 we show, for example, the predictions of the CONFLOW model (Mastin, 2002) for three cases: 1) the effect of bubbles is not considered; 2) bubbles are considered and flow is assumed to be in regime 1 (minimum model) throughout the conduit; 3) flow is assumed to be in regime 2 (minimum model) throughout the conduit. All other parameters are the same for all three calculations. Despite using the minimum rheological model, the inferred fragmentation depth for these three cases varies by $\approx$ 800m, indicating that the influence of bubbles on fragmentation depth in the real world is at least this strong and probably much stronger.

Elsewhere in this volume, Starostin *et al.* present a conduit flow model which calculates the effect of bubbles on rheology after the method proposed in this paper. Again, in this case the minimum model is used and the eruption rate for an explosive eruption is plotted as a function of time for three cases: 1) the effect of bubbles is not considered; 2) the effect of bubbles is considered and an initial bubble number-density of $10^{15}\mathrm{m}^{-3}$ is assumed (equivalent to specifying small bubbles); 3) the effect of bubbles is considered and an initial bubble number-density of $10^{9}\mathrm{m}^{-3}$ is assumed (equivalent to specifying large bubbles). An increase in peak discharge rate of almost 10% and an increase in flow-rate of almost 20% after 3 minutes is

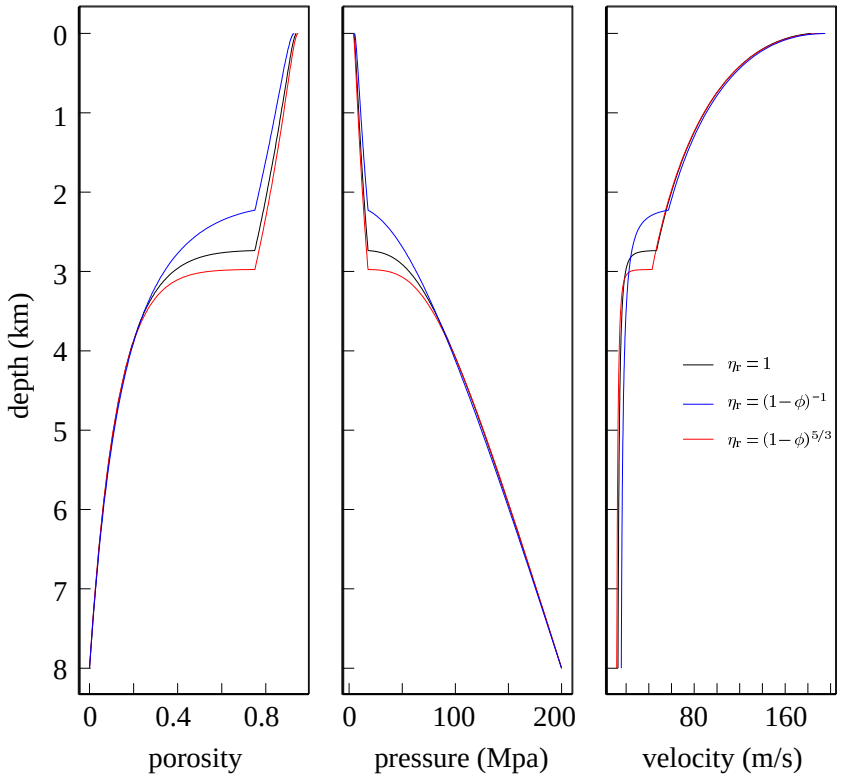

FIGURE 5. Porosity, pressure and vertical velocity against depth in a volcanic conduit calculated using CONFLOW (Mastin, 2002). The black line ignores the effect of bubbles on viscosity, the blue line considers the effect of bubbles and assumes that flow is in regime 1 (minimum model) throughout the conduit, the red line considers the effect of bubbles and assumes that flow is in regime 2 (minimum model) throughout the conduit. In each case the fragmentation depth is indicated by the inflection point in the curve. It can be seen that, even for the minimum rheological model, the effect of bubbles on the magma's rheology has a profound influence on fragmentation depth.

observed. Again, considering that this model assumes the minimum rheological model presented in this paper, it is likely that the influence of bubbles on discharge rate in the real world is at least as strong as this and probably much stronger.

5. Concluding remarks

The conduit model predictions shown in figures 5 and 6 highlight the importance of accounting for the effects of bubbles on rheology. We note, however, that both our discussion and current conduit models address only one aspect of the effect of bubbles on conduit flow dynamics: the effect on shear viscosity. Other effects, such as non-zero normal stresses, introduction of a bulk (compressible) viscosity, bubble

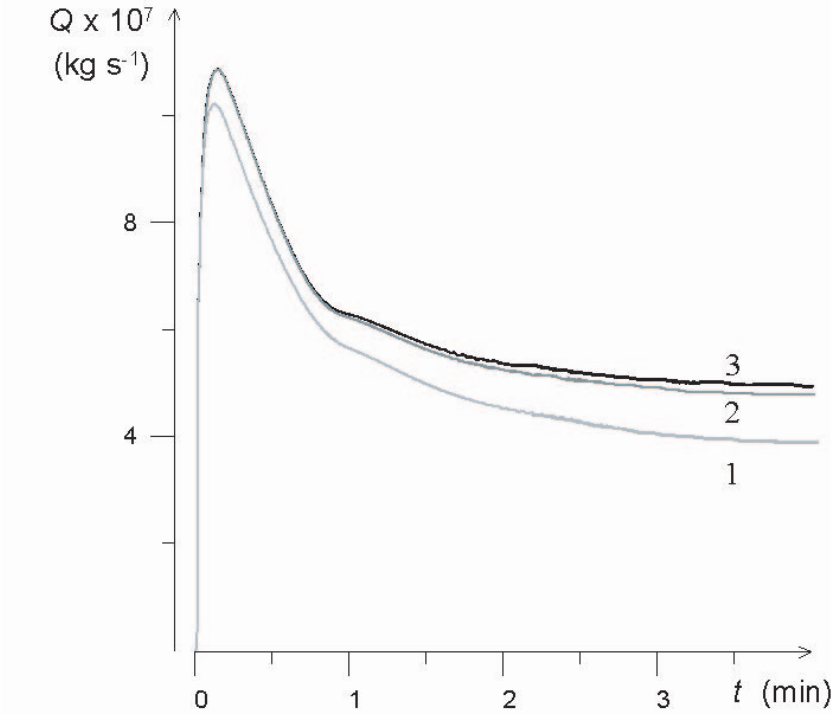

FIGURE 6. Eruption rate over time for an explosive eruption using the model of Starostin *et al.* presented elsewhere in this volume. The light grey line ignores the effect of bubbles, the dark grey line considers the effect of bubbles and assumes an initial bubble number-density of $10^{15}\mathrm{m}^{-3}$, the black line considers the effect of bubbles and assumes an initial bubble number-density of $10^{9}\mathrm{m}^{-3}$. It is evident that, even for the minimum rheological model, the effect of bubbles on the magma's rheology has a profound influence on eruption rate.

coalescence and breakup etc. may also have a significant effect on conduit flow dynamics. In addition, some of the subtlety of the effect of bubbles on shear viscosity has been sacrificed for simplicity of implementation. It is believed, however, that the method outlined here captures the salient features of bubble rheology. There is still some disagreement between experimental studies on bubble suspension rheology, highlighted at the end of section 2.3; one of the strengths of the implementation presented in these notes is that equations 7 and 8 can be adapted easily as improved experimental data become available.

The algorithmic approach to incorporating the effect of bubbles on the shear viscosity of magma in a conduit flow model is intended as a guide only. It is expected that some deviation from this procedure will be necessary for certain classes of model.

References

[1] Hinch E.J. and Acrivos A., 1980. Long slender drops in a simple shear flow. *J. Fluid Mech.* **98**, 305-328.

[2] Bagdassarov N.S. & Dingwell D.B., 1992. A rheological investigation of vesicular rhyolite. *J. Volcanol. Geotherm. Res.*, **50**, 307–322.

[3] Bagdassarov N.S. & Dingwell D.B., 1993. Frequency dependent rheology of vesicular rhyolite. *J. Geophys. Res.*, **98**, 6477–6487.

[4] Batchelor G.K., 1970. The stress system in a suspension of force-free particles. *J. Fluid Mech.* **41** 545-470.

[5] Brinkman H.C., 1952. The viscosity of concentrated suspensions and solutions. *J. Chem. Phys.*, **20**, 571.

[6] Cristini V., Macosko C.W. and Jansseune T., 2002. A note on the transient stress calculation via numerical simulations. *J. nonNewt. Fluid Mech.*, **105**, 177-187.

[7] Ducamp V.C. & Raj R., 1989. Shear and densification of glass powder compacts. *J. Am. Ceram. Soc*, **72**, 798–804.

[8] Frankel N.A. & Acrivos A., 1970. The constitutive equation for a dilute emulsion. *J. Fluid Mech.*, **44**, 65–78.

[9] Hu Y.T. & Lips A., 2003. Transient and steady state three-dimensional drop shapes and dimensions under planar extensional flow. *J. Rheology* **47**, 349–369.

[10] Jackson, N.E. and Tucker, C.L., 2003, A model for large deformation of an ellipsoidal droplet with interfacial tension. *J. Rheology*, **47**, 659-682.

[11] Jansseune, T. Vinckier I. Moldernaers P. and Mewis J., 2001. Transient stresses in immiscible polymer blends during start-up flows. *J. nonNewt. Fluid Mech.*, **99**, 167-181.

[12] Lejeune A.M., Bottinga Y., Trull T.W. & Richet P., 1999. Rheology of bubble-bearing magmas. *Earth Planet. Sci. Lett.*, **166**, 71–84.

[13] Llewellin E.W., Mader H.M. & Wilson S.D.R., 2002a. The rheology of a bubbly liquid. *Proc. Roy. Soc. A*, **458**, 987–1016.

[14] Llewellin E.W., Mader H.M. & Wilson S.D.R., 2002b. The constitutive equation and flow dynamics of bubbly magmas. *Geophys. Res. Lett.*, **29**, art. no. 2170.

[15] Loewenberg M. & Hinch E.J., 1996. Numerical simulation of a concentrated emulsion in shear flow. *J. Fluid Mech.*, **321**, 395–419.

[16] Mackenzie J.K., 1950. The elastic constants of a solid containing spherical holes. *Proc. Roy. Soc. A*, **63**, 2–11.

[17] Maffettone, P.L. and Minale M., 1998. Equation of change of ellipsoidal drops in viscous flow. *J. nonNewt. Fluid Mech.*, **78**, 227-241.

[18] Manga M., Castro J., Cashman K. & Loewenberg M., 1998. Rheology of bubble-bearing magmas. *J. Volcanol. Geotherm. Res.*, **87**, 15–28.

[19] Mastin, L.G., 2002, Insights intro volcanic conduit flow from an open-source numerical model, *Geochm., Geophys., Geosys.*, **3**: 10.1029.

[20] Manga M. & Loewenberg M., 2001. Viscosity of magmas containing highly deformable bubbles. *J. Volcanol. Geotherm. Res.*, **105**, 19–24.

[21] Murase T. & McBirney R., 1973. Properties of some common igneous rocks and their melts at high temperatures. *Geol. Soc. Am. Bull.*, **84**, 3563–3592.

[22] Oldroyd J.G., 1953. The elastic and viscous properties of emulsions and suspensions. *Proc. Roy. Soc. A*, **218**, 122–132.

[23] Oosterbroek M. & Mellema J., 1981. Linear viscoelasticity in emulsions. I. The effect of an interfacial film on the dynamic viscosity of nondilute emulsions. *J. Colloid Interface Sci.*, **84**, 14–26.

[24] Pal R., 2003. Rheological behaviour of bubble-bearing magmas. *Earth Planet. Sci. Lett.*, **207**, 165–179.

[25] Rahaman M.N., De Jonghe L.C., Scherer G.W. & Brook R.J., 1987. Creep and densification during sintering of glass powder compacts. *J. Am. Ceram. Soc*, **70**, 766–774.

[26] Roscoe R., 1952. The viscosity of suspensions of rigid spheres. *Brit. J. Appl. Phys.*, **2**, 267–269.

[27] Rust A.C. & Manga M., 2002a. Effects of bubble deformation on the viscosity of dilute suspensions. *J. Non-Newtonian Fluid Mech.*, **104**, 53–63.

[28] Rust A.C. & Manga M., 2002b. Bubble shapes and orientations in low Re simple shear flow. *J. Colloid Interface Sci.*, **249**, 476–480.
[29] Rust A.C., Manga M. & Cashman K.V., 2003. Determining flow type, shear rate and shear stress in magmas from bubble shapes and orientations. *J. Volcanol. Geotherm. Res.*, **122**, 111–132.
[30] Schowalter W.R., Chaffey C.E., & Brenner H., 1968. Rheological behaviour of a dilute emulsion. *J. Colloid. Int. Sci.*, **26**, 152–160.
[31] Starostin et al (elsewhere in this volume)
[32] Stein D.J. & Spera F.J., 1992. Rheology and microstructure of magmatic emulsions: theory and experiments. *J. Volcanol. Geotherm. Res.*, **49**, 157–174.
[33] Stein D.J. & Spera F.J., 2002. Shear viscosity of rhyolite–vapour emulsions at magmatic temperatures by concentric cylinder rheometry. *J. Volcanol. Geotherm. Res.*, **113**, 243–258.
[34] Taylor G.I., 1932. The viscosity of a fluid containing small drops of another fluid. *Proc. Roy. Soc. A*, **138**, 41–48.
[35] Taylor G.I., 1934. The formation of emulsions in definable fields of flow. *Proc. Roy. Soc. Lond. A*, **146**, 501-523.
[36] Tucker C.L. and Moldenaers P., 2002. Microstructural evolution in polymer blends. *Ann. Rev. Fluid Mech.*, **34**, 177-210.
[37] Yu, W. and Bousmina, M., 2003. Ellipsoidal model for droplet deformation in emulsions. *J. Rheol.*, **47**. 1011-1039.
[38] Wu Y., Zinchenko, A.Z. and Davis R.H., 2002. Ellipsoidal model for deformable drops and application to nonNewtonian emulsion flow. *J. NonNewtonian Fluid Mech.*, **102**, 281-298.

(Ed Llewellin) University of Bristol, UK
E-mail address: ed.llewellin@bris.ac.uk

(Michael Manga) University of California, Berkeley, USA
E-mail address: manga@seismo.berkeley.edu